Robotica (2017) volume 35, pp. 1923–1938. © Cambridge University Press 2016
doi:10.1017/S0263574716000588

Robust task-space control of robot manipulators using differential equations for uncertainty estimation

Alireza Izadbakhsh†,* and Saeed Khorashadizadeh‡

†*Department of Electrical Engineering, College of Engineering, Garmsar branch, Islamic Azad University, Garmsar, Iran*
‡*Department of Electrical Engineering, Faculty of Engineering, University of Birjand, Birjand, Iran*
E-mail: s_khorashadi@yahoo.com

(Accepted July 21, 2016. First published online: September 8, 2016)

SUMMARY
Most control algorithms for rigid-link electrically driven robots are given in joint coordinates. However, since the task to be accomplished is expressed in Cartesian coordinates, inverse kinematics has to be computed in order to implement the control law. Alternatively, one can develop the necessary theory directly in workspace coordinates. This has the disadvantage of a more complex robot model. In this paper, a robust control scheme is given to achieve exact Cartesian tracking without the knowledge of the manipulator kinematics and dynamics, actuator dynamics and nor computing inverse kinematics. The control design procedure is based on a new form of universal approximation theory and using Stone–Weierstrass theorem, to mitigate structured and unstructured uncertainties associated with external disturbances and actuated manipulator dynamics. It has been assumed that the lumped uncertainty can be modeled by linear differential equations. As the method is Model-Free, a broad range of manipulators can be controlled. Numerical case studies are developed for an industrial robot manipulator.

KEYWORDS: Model-free control, Electrically driven robot manipulator, Differential equations, Robust control.

1. Introduction

Over the past decades, robust control of robot manipulators has been studied extensively and many control schemes have been proposed in the literature.[1–4] These conventional robust non-linear controllers are based on nominal models. Usually, the proposed nominal models have the same structure as the actual models. Consequently, the lengthy and tedious regressor analysis is inevitable in traditional robust and adaptive control methodologies,[5] since these approaches are based on the linear parameterization of the manipulator dynamics. Sensing requirements are another challenge in this field. Most of the presented algorithms need the velocity feedback and some of them require the acceleration feedback. The acceleration signal is usually contaminated with noise and may degrade the controller performance. Moreover, many commercial robots provide the user with only joint position measurements. Thus, practical implementation of these controllers may be impossible or too expensive. In some robust control strategies such as sliding mode control,[6] the uncertainty upper bound should be known in advance or estimated. If the estimated bound is greater than its actual value, the control system will face saturation of input and the chattering phenomenon, while too low estimation of the bound may cause a higher tracking error.

To solve the aforementioned problems, various adaptive fuzzy systems[7,8] and neural networks[9] have been used in robust control of robot manipulators, since according to the universal approximation theorem,[10] they can estimate non-linear functions with arbitrary small approximation error.

*Corresponding author. E-mail: izadbakhsh_alireza@hotmail.com

https://doi.org/10.1017/S0263574716000588 Published online by Cambridge University Press

Fault-tolerance, parallelism and excellent learning capabilities are other beneficial characteristics of fuzzy systems and neural networks.[11] The unknown parameters in the structure of neural networks and fuzzy systems are adjusted online using some adaptation laws derived from a Lyapunov-based stability analysis. Sometimes, designing a satisfactory fuzzy controller for a complicated system requires the knowledge of some experts specialized in that field. Without this vital information, designing a proper fuzzy controller may be a tedious task due to the time-consuming trial and error procedure. Moreover, neuro-fuzzy estimators require various feedbacks for their inputs. For example, if the uncertainty is a function of some state variables, all those states should be available and fed to the fuzzy system or neural network as inputs. As a result, the control law may become computational. In addition, usually the projection algorithm is needed to make the adjustable parameters of neural networks and fuzzy systems limited to pre-defined regions, which can impose extra computational burden to the processor. Moreover, the structure of neural network and its parameters are important issues which should be determined carefully.

Recently, some regressor-free approaches have been presented[12–19] in which uncertainties have been approximated using Legendre polynomials or the Fourier series expansion. On the basis of Lyapunov stability, some adaptation laws are derived for adjustment of the Fourier series/Legendre coefficients. In comparison with neuro-fuzzy controllers, these approaches are superior in some ways:

(1) First, they can considerably reduce the number of required feedbacks.[19] In neuro-fuzzy approaches, providing the controller with some of these feedbacks may be impossible or expensive, while in regressor-free approaches, the Fourier series expansion or Legendre polynomials are used for uncertainty estimation which do not require various feedbacks. The reason is that these estimators consider the uncertainty as a time-varying function rather than a function of different state variables.
(2) Second, applying regressor-free approaches to robust control is very simple and there are very fewer tuning parameters in the Fourier series expansion or Legendre polynomials.

Recently, some observer–controller structures have been proposed in which unmeasurable signals are estimated.[20] In comparison with these strategies, regressor-free approaches are superior, since there is no need to assume that uncertainty is constant or varies slowly. Moreover, the uncertainty bound is not required in regressor-free approaches. This bound is selected using the trial and error procedure which is time consuming or estimated online.

Motivated by the aforementioned advantages of regressor-free approaches, this paper develops a novel robust model-free algorithm for task-space control of electrically driven robot manipulators. It is assumed that the lumped uncertainty can be modeled by a linear differential equation. Also, the modeling error is compensated. The control law is a simple state feedback accompanied by a compensator to overcome uncertainties and modeling error.

In comparison with previous related works in the task-space,[21] the design procedure for this controller is simpler, since there is no need to determine the regressor matrix or propose a nominal model for the manipulator. In comparison with other robust algorithms,[1,2] the proposed controller is superior from different points of view. Due to the discontinuous control laws in refs. [1, 2], the chattering phenomenon is possible in these approaches and a solution is required to attenuate it. In addition, there are some parameters related to uncertainty upper bound in these strategies, which should be tuned using trial and error, while the proposed method is free from uncertainty upper bound.

Nowadays, actuator dynamics are usually included in the design procedure of robot manipulators[22–24] and motor voltages are considered as the control efforts. These approaches are referred as voltage-based controllers. The control law in computed torque approaches[1] cannot be applied to the robotic system directly.[19] As a result, from practical point of view, voltage-based methods are preferable. Therefore, in this paper, a robust model-free voltage-based controller is presented.

This paper is organized into six sections. Following the introduction, in Section 2, a task-space dynamic model for electrically driven robots is presented. Section 3 presents the proposed control law. Stability analysis is given in Section 4. Section 5 illustrates the simulation results using a Puma560 manipulator and finally, conclusions are drawn in Section 6.

https://doi.org/10.1017/S0263574716000588 Published online by Cambridge University Press

2. Mathematical Model

In the following subsections, we derive the kinematic and dynamic model of an n-DOF robot manipulator with revolute joints. The manipulator is supposed to move in three-dimentional space.[22]

2.1. Dynamic analysis

Dynamic equations of a rigid-link electrically driven robot manipulator with n degrees of freedom are described as

$$D(q)\ddot{q} + C(q,\dot{q})\dot{q} + g(q) + F(\dot{q}) + T_l(t) = \tau_l, \tag{1}$$

$$J_m\ddot{\theta} + B\dot{\theta} = K_m I - r\tau_l, \tag{2}$$

$$L\dot{I} + RI = u(t) - K_b\dot{\theta}, \tag{3}$$

where $q \in \Re^n$ is the vector of generalized joint coordinates, $D(q) \in \Re^{n\times n}$ is the symmetric positive definite inertia matrix including the added mass effects, $C(q,\dot{q})\dot{q} \in \Re^n$ is the vector of Coriolis and centrifugal generalized forces, $g(q) \in \Re^n$ denotes the gravitational force vector, $F(\dot{q}) \in \Re^n$ is the static and dynamic friction terms, $T_l(t) \in \Re^n$ is the vector of disturbance torques, $\tau_l \in \Re^n$ is the vector of load torques applied on motor shaft, $\theta \in \Re^n$ is the vector of motor angular positions, $J_m \in \Re^{n\times n}$ is the diagonal matrix of the lumped actuator rotor inertia along with the motor side elements of the transmission, $B \in \Re^{n\times n}$ denotes the diagonal matrix of the lumped actuator damping coefficients and motor side elements of the transmission, $K_m \in \Re^{n\times n}$ is the motor torque transmission constant matrix which characterizes the electromechanical conversion between current and torque, $I \in \Re^n$ is the vector of armature currents, $L \in \Re^{n\times n}$ represents the actuator inductance matrix, $R \in \Re^{n\times n}$ is the actuator resistance matrix, $K_b \in \Re^{n\times n}$ is the matrix characterizing back EMF constants of the actuator, $u(t) \in \Re^n$ denotes the vector of armature voltages applied to the joint actuators and r is the $n \times n$ transmission matrix, which maps the $n \times 1$ vector of motor angular velocities, $\dot{\theta}$, to the vector of generalized joint coordinate velocities, $\dot{q}$, as

$$\dot{q} = r\dot{\theta}. \tag{4}$$

Substituting Eq. (4) into Eqs. (2) and (3), we can write

$$J_m r^{-1}\ddot{q} + Br^{-1}\dot{q} = K_m I - r\tau_l, \tag{5}$$

$$L\dot{I} + RI = u(t) - K_b r^{-1}\dot{q}, \tag{6}$$

where L, K_b, R and K_m are positive definite constant diagonal matrices. It is worth noting that in all practically well-designed actuators, the armature inductance L is small. Thus, for small enough $L > 0$, Eqs. (5) and (6) govern a singularly perturbed system, in which I and q are the fast and slow variables, respectively.[22] By setting $L = 0$ in Eq. (6), solving it for I, and substituting I into Eq. (5), we can write

$$RK_m^{-1}J_m r^{-1}\ddot{q} + (RK_m^{-1}B + K_b)r^{-1}\dot{q} = u(t) - RK_m^{-1}r\tau_l. \tag{7}$$

Substitution of Eq. (1) into (7) yields the following overall dynamic of electrically driven robot:

$$\bar{D}(q)\ddot{q} + \bar{C}(q,\dot{q})\dot{q} + \bar{G}(q) = u(t) \tag{8}$$

in which

$$\begin{aligned} \bar{D}(q) &= RK_m^{-1}(J_m r^{-1} + rD(q)), \\ \bar{C}(q,\dot{q}) &= RK_m^{-1}(Br^{-1} + rC(q,\dot{q})) + K_b r^{-1}, \\ \bar{G}(q) &= RK_m^{-1}r(g(q) + F(\dot{q}) + T_l(t)). \end{aligned} \tag{9}$$

https://doi.org/10.1017/S0263574716000588 Published online by Cambridge University Press

2.2. Kinematic analysis

With respect to n-joint coordinates q , and m task coordinates h , the kinematics of the manipulator can be described with the following equations:[25]

$$h = \phi(q), \tag{10}$$

$$\dot{h} = J(q)\dot{q}, \tag{11}$$

$$\ddot{h} = J(q)\ddot{q} + \dot{J}(q)\dot{q}, \tag{12}$$

where ϕ is an m-dimensional vector function representing direct kinematics, $J(q) \in \Re^{m\times n}$ is the Jacobian matrix defined as $\partial\phi/\partial q$ and the upper dot denotes its time derivative. The two last equations are known as the first- and second-order differential kinematics, respectively. With this in mind, the equation for robot system motion in the joint space, Eq. (8), can then be represented as Cartesian space coordinates based on the following relationship:

$$\ddot{q} = J(q)^{-1}(\ddot{h} - \dot{J}(q)\dot{q}). \tag{13}$$

Substituting Eq. (13) into (8) yields

$$M(h)\ddot{h} + N(h, \dot{h})\dot{h} + G(h) = v(t), \tag{14}$$

where

$$\begin{aligned} M(h) &= J(q)^{-T}\bar{D}(q)J(q)^{-1}, \\ N(h, \dot{h}) &= J(q)^{-T}\left(\bar{C}(q, \dot{q}) - \bar{D}(q)J(q)^{-1}\dot{J}(q)\right)J(q)^{-1}, \\ G(h) &= J(q)^{-T}\bar{G}(q), \\ v(t) &= J(q)^{-T}u(t). \end{aligned} \tag{15}$$

As can be seen form Eqs. (14) and (15), the mathematical relation between the operational space pose (position and orientation) and control inputs, contains the time derivative, inverse as well as transpose transformation of the Jacobian matrix, that can burden the control system and reduce its performance. Thus, controller design for such highly non-linear dynamics is generally complex and computationally difficult due to complexity or uncertainties in $M(h)$,$N(h, \dot{h})$ and $G(h)$. This problem becomes hypersensitive especially for higher DOF actuated robotic manipulators. The control objective for the robotic system is hence to drive the manipulator endpoint to follow a desired trajectory defined in task space, in the presence of possibly large (but bounded) and unknown uncertainties in the system kinematics, manipulator dynamics and actuators. Toward this end, we can represent Eq. (14) in the form of:[22]

$$m_{ii}(h)\ddot{h}_i + n_i(h, \dot{h})\dot{h}_i + g_i(h) \; + \sum_{j=1,\, j\neq i}^{n} m_{ij}(h)\ddot{h}_j = v_i(t)\,\{i= 1, 2,...,n\}\,, \tag{16}$$

where the subscript "i" indicates the ith element, and $m_{ii}(h)$ is the varying effective inertia seen at the ith joint, $n_i(h, \dot{h})\dot{h}_i$ is the ith element of $N(h, \dot{h})\dot{h}$, $g_i(h)$ is the ith element of $G(h)$ and $v_i(t)$ is the ith element of $v(t)$. In fact, Eq. (16) is the ith row of Eq. (14). It can easily be shown that Eq. (16) can also be rewritten as

$$\dot{x} = Ax + Bv_i(t) + B\delta, \tag{17}$$

$$y = Cx, \tag{18}$$

https://doi.org/10.1017/S0263574716000588 Published online by Cambridge University Press

where

$$x = [\, h_i \;\; \dot{h}_i \,]^T, \;\; A = \begin{bmatrix} 0 & 1 \\ 0 & 0 \end{bmatrix}, \;\; B = \begin{bmatrix} 0 \\ 1 \end{bmatrix}, \;\; C = [\, 1 \; 0 \,],$$
$$\delta = m_{ii}^{-1}(h)((1 - m_{ii})v_i(t) - n_i(h, \dot{h})\dot{h}_i - g_i(h) - \sum_{j=1,\, j \neq i}^{n} m_{ij}(h)\ddot{h}_j). \tag{19}$$

3. Control Design

With regards to the former, a robust task-space control strategy is developed that eliminates elaboration and computational burden inherent in a conventional task-space control strategy. Toward this end, consider the following assumptions:

Assumption 1. The manipulator is operating away from any singularity.

Assumption 2. If δ (constant or time varying) represents uncertainties that include inertia, Coriolis/centrifugal forces, gravity force, external disturbances, unmodeled dynamics and kinematic uncertainties, $\delta \in T$, where T is a compact set.

Under the assumption of unknown system dynamics structure, and unknown geometric and mass properties, a control law is developed as

$$v_i(t) = -kx + k_0 r. \tag{20}$$

Substituting Eq. (20) into (17) gives

$$\dot{x} = (A - Bk)x + Bk_0 r + B\delta. \tag{21}$$

Now, we design an algorithm to adjust the control input r such that the task-space tracking error is reduced even in the presence of uncertainties. To this end, a desired closed-loop state-space equation is defined as

$$\dot{x}_d = (A - Bk)x_d + Bk_0 r_d, \tag{22}$$
$$y_d = Cx_d, \tag{23}$$

where r_d and y_d are the input and output corresponding to x_d. As a result, using Eqs. (22) and (23), the control gains can be selected in a more systematic manner. Once the motion specification is given in terms of the desired trajectory r_d in the operational space, then the motion control objective in operational space is to achieve

$$\lim_{t \to \infty} \xi(t) = 0, \tag{24}$$

where

$$\xi(t) = y(t) - y_d(t) \tag{25}$$

denotes the operational space pose error (position and orientation). Then, the system error dynamics becomes

$$\dot{\tilde{x}}(t) = (A - Bk)\tilde{x}(t) + Bk_0\psi(t) + B\delta, \tag{26}$$
$$\xi(t) = C\tilde{x}(t), \tag{27}$$

https://doi.org/10.1017/S0263574716000588 Published online by Cambridge University Press

where

$$\psi(t) = r(t) - r_d(t) \tag{28}$$

and $\tilde{x}(t)$ is defined as $\tilde{x}(t) = x(t) - x_d(t)$.

Assumption 3. The desired reference trajectory r_d is assumed to be bounded and uniformly continuous, and has bounded and uniformly continuous derivatives up to a necessary order.

To determine the influence of input $\psi(t)$ on the tracking error, Eqs. (26) and (27) are differentiated p-times to obtain

$$\dot{\wp}(t) = (A - Bk)\wp(t) + Bk_0\vartheta(t) + B\lambda(t), \tag{29}$$

$$\xi^{(p)}(t) = C\wp(t) + \sum_{j=1}^{p} b_j \xi^{(p-j)}, \tag{30}$$

where

$$\wp(t) = \tilde{x}^{(p)} - \sum_{j=1}^{p} b_j \tilde{x}^{(p-j)}, \tag{31}$$

$$\vartheta(t) = \psi^{(p)} - \sum_{j=1}^{p} b_j \psi^{(p-j)}, \tag{32}$$

and $\lambda(t)$ is the lumped approximation error. In other words, it has been supposed that, uncertainties can be approximated by a p-th order ordinary differential equation of the form:[26–28]

$$\delta^{(p)} - \sum_{j=1}^{p} b_j \delta^{(p-j)} = 0, \tag{33}$$

where the order p reflects the dynamic structure of δ , and b_j 's are zero or positive real scalars to be designed. It should be emphasized that in Eqs. (30)–(33), the coefficients b_j 's are the same. This approximation opens the possibility to obtain the corrective input $\vartheta(t)$ to include it into the controller to compensate the perturbation present in the plant.

Remark 1. Equation (33) is a p-th order ordinary differential equation. It can be easily shown that the solution of this equation is a continuous function as

$$\delta(t) = \sum_{i=1}^{p} c_i \mathrm{e}^{\lambda_i t} Cos\left(\omega_i t + \theta_{\delta_i}\right), \tag{34}$$

where c_i , λ_i , ω_i and θ_{δ_i} are unknown constants depending on the lumped uncertainty $\delta(t)$. It is interesting to investigate the capability of the last assumption, Eq. (33), from a function approximation capability point of view. Herein, we will prove that Eq. (34) have the universal approximation capability. In the following, we suppose that the input universe of discourse T is a convex set in $\Re$. First, we need the following useful theorem.

Stone–Weierstrass theorem.[29] It seems that Marshall H. Stone has been the first researcher who formulated the new universal approximation theorem (https://en.wikipedia.org/wiki/Stone%E2%80%93Weierstrass_theorem). Let o be a set of real continuous functions on a convex set T. If

(1) the set o is algebra, that is the set o is closed under multiplication, addition, and scalar multiplication;

https://doi.org/10.1017/S0263574716000588 Published online by Cambridge University Press

(2) the set o separates points of T, i.e.

$$\forall t_1,\ t_2 \in T, t_1 \neq t_2, \exists\, \delta(t) \in o : \delta(t_1) \neq \delta(t_2). \tag{35}$$

Note that the variable "t" means time and the dimension of the convex set "T" is one.

(3) The set o vanishes at no point of T, that is,

$$\forall t \in T, \exists \delta(t) \in o :\ \delta(t) \neq 0, \tag{36}$$

then for any real continuous function $\delta(t)$ on T and arbitrary $\varepsilon > 0$, there exists a function $f(t)$ in o such that

$$\underset{t\in T}{Sup}\, |f(t) - \delta(t)| < \varepsilon. \tag{37}$$

Proposition 1 (Universal approximation theorem)**.** Let $\delta(t)$ be a continuous real function on the convex set T in $\Re$. Then, for each arbitrary $\varepsilon > 0$, there exists a function in the form of

$$\sum_{i=1}^{p} c_i e^{\lambda_i t} Cos\left(\omega_i t + \theta_{\delta_i}\right) \tag{38}$$

such that

$$\underset{t\in T}{Sup} \left| \sum_{i=1}^{p} c_i e^{\lambda_i t} Cos\left(\omega_i t + \theta_{\delta_i}\right) - \delta(t) \right| < \varepsilon. \tag{39}$$

Proof of Proposition 1. Let o to be a set of continuous function on T in which T is a Convex set in the form of Eq. (34). Now, suppose $\delta_1(t)$ and $\delta_2(t)$ are given as

$$\begin{aligned} \delta_1(t) &= \sum_{i=1}^{p} c_i e^{\lambda_i t} Cos\left(\omega_i t + \theta_{\delta_i}\right), \\ \delta_2(t) &= \sum_{j=1}^{p} \bar{c}_j e^{\bar{\lambda}_j t} Cos\left(\bar{\omega}_j t + \bar{\theta}_{\delta_j}\right), \end{aligned} \tag{40}$$

we have

$$\begin{aligned} \delta_1(t) + \delta_2(t) &= \sum_{i=1}^{p} c_i e^{\lambda_i t} Cos\left(\omega_i t + \theta_{\delta_i}\right) + \sum_{j=1}^{p} \bar{c}_j e^{\bar{\lambda}_j t} Cos\left(\bar{\omega}_j t + \bar{\theta}_{\delta_j}\right), \\ \delta_1(t).\delta_2(t) &= \frac{1}{2} \sum_{i=1}^{p} \sum_{j=1}^{p} c_i \bar{c}_j e^{(\lambda_i + \bar{\lambda}_j)t} Cos\left(\left(\omega_i + \bar{\omega}_j\right) t + \left(\theta_{\delta_i} + \bar{\theta}_{\delta_j}\right)\right) \\ &\quad + \frac{1}{2} \sum_{i=1}^{p} \sum_{j=1}^{p} c_i \bar{c}_j e^{(\lambda_i + \bar{\lambda}_j)t} Cos\left(\left(\omega_i - \bar{\omega}_j\right) t + \left(\theta_{\delta_i} - \bar{\theta}_{\delta_j}\right)\right). \end{aligned} \tag{41}$$

Hence, $\delta_1(t) + \delta_2(t) \in o$ and $\delta_1(t).\delta_2(t) \in o$. Finally, for any arbitrary $\sigma \in \Re$, we can get

$$\sigma.\delta(t) = \sum_{i=1}^{p} \sigma c_i e^{\lambda_i t} Cos\left(\omega_i t + \theta_{\delta_i}\right) \tag{42}$$

https://doi.org/10.1017/S0263574716000588 Published online by Cambridge University Press

which is also in the form of Eq. (34). So, according to Eqs. (41) and (42), we can conclude that o is an algebra. Therefore, the first condition of the Stone–Weierstrass theorem is satisfied for o. Now, we show that o separates various points on T. Choose the parameters of $\delta(t)$ in Eq. (34) as

$$c_1 = 1, \ \ \lambda_1 = -1, \ \omega_1 = 0, \ \theta_{\delta_1} = 0. \tag{43}$$

Since $t_1 \neq t_2$, then $e^{-t_1} \neq e^{-t_2}$, therefore the second condition is also verified. To show that o vanishes at no point of T, we simply observe that any function in the form of Eq. (34) with $\omega_i = 0$, $\theta_{\delta i} = 0$ and $c_i > 0$ has the property of

$$\forall t \in T, \delta(t) > 0. \tag{44}$$

Hence, o vanishes at no point of T. Thus, the three conditions of the Stone–Weierstrass theorem are satisfied. Therefore, the result follows by Stone–Weierstrass theorem. □

Remark 2. It should be noted that **Proposition 1** proves only the existence result. That is, we can always find the parameters p, b_j, c_i, ω_i and λ_i which can approximate any continuous function with arbitrary small approximation error, such that the assumption (33) is satisfied. In other words, it implies that there exist the parameters p and b_j that validate Eq. (33) for approximation of unknown disturbance dynamics. However, the appropriate values for the order p and the coefficients b_j depend mainly on the trial and error related to the application's type. For our systems under study, it has been shown that even $p = 1$ yields good results. The validity of the proposed approach will be verified with some simulation results on a six-DOF industrial robot.

Now, we can define a coordinate transformation represented by

$$Z = [\xi \ \dot{\xi} \ \ldots \ \xi^{(p-1)} \ \wp(t)]^T. \tag{45}$$

Then, the system state equation in new coordinates will be

$$\dot{Z} = \Lambda Z + \Psi \vartheta(t) + \Xi, \tag{46}$$

$$y = HZ, \tag{47}$$

where

$$\begin{aligned} \Lambda &= \begin{bmatrix} 0 & 1 & 0 & \cdots & 0 & 0 \\ 0 & 0 & 1 & \cdots & 0 & 0 \\ \vdots & \vdots & \vdots & \vdots & \vdots & \vdots \\ 0 & 0 & \cdots & \cdots & 1 & 0 \\ b_p & b_{p-1} & \cdots & \cdots & b_1 & C \\ 0 & 0 & \cdots & \cdots & 0 & A - Bk \end{bmatrix}, \\ \Psi &= \begin{bmatrix} 0 & \cdots & 0 \ (Bk_0)^T \end{bmatrix}^{\mathrm{T}}, \Xi = \begin{bmatrix} 0 \cdots 0 \ (B\dot{\lambda}(t))^T \end{bmatrix}^{\mathrm{T}}, \\ H &= \begin{bmatrix} 1 \, 0 \cdots 0 \end{bmatrix}, \end{aligned} \tag{48}$$

and $\vartheta(t)$ is defined as

$$\vartheta(t) = -\mu Z \tag{49}$$

such that the satisfactory performance of Cartesian trajectory tracking is obtained. It should be mentioned that, although ξ is a function of the tracking error $\tilde{x}(t)$, $\vartheta(t)$ depends on the tracking error. The final step is to adjust the control input in Eq. (28) to account for the effects of modeling errors and external disturbance as

$$r(t) = r_d(t) + \psi(t), \tag{50}$$

https://doi.org/10.1017/S0263574716000588 Published online by Cambridge University Press

where $\psi(t)$ is the auxiliary control input. The last equation says that the control input must be modified as Eq. (50) to have a high accuracy motion in the response of unwanted uncertainties. More precisely, the robot should be controlled to follow the modified signal $r(t)$, instead of $r_d(t)$. If this modification is violated, the tracking error may never converge to zero.

4. Stability Analysis

To study the stability and analyze the performances of closed-loop system (46), consider the following Lyapunov function candidate:

$$V = Z^T P Z \tag{51}$$

in which $P = P^T$ is a positive definite matrix satisfying the Lyapunov equation $(\Lambda - \Psi\mu)^T P + P(\Lambda - \Psi\mu) = -Q$, where Q is a positive definite matrix. Taking the time derivative of Eq. (51) along the trajectories of Eqs. (46) and (49), we have

$$\dot{V} \leq -\lambda_{\min}(Q)\|Z\|^2 + 2\lambda_{\max}(P)\,\|Z\|\,\|\Xi\|\,, \tag{52}$$

where $\lambda_{\min}(Q)$ and $\lambda_{\max}(P)$ denote the minimum and maximum eigenvalues of Q and P , respectively.

Remark 3. Suppose that the appropriate models are used and the approximation error can be ignored. Then, $\dot{V}$ is negative definite, and the asymptotic stability of the closed-loop system can be approved.

Remark 4. If the approximation error cannot be ignored, after some further manipulations of Eq. (52), we have

$$\begin{aligned}\dot{V} \leq & -\frac{1}{2}\left(\sqrt{\lambda_{\min}(Q)}\,\|Z\| - 2\frac{\lambda_{\max}(P)\,\|\Xi\|}{\sqrt{\lambda_{\min}(Q)}}\right)^2 \\ & - \frac{1}{2}\left(\lambda_{\min}(Q)\|Z\|^2 - 4\frac{\lambda_{\max}^2(P)\|\Xi\|^2}{\lambda_{\min}(Q)}\right)\end{aligned} \tag{53}$$

which can also be expressed as

$$\dot{V} \leq \underbrace{-\frac{1}{2}\lambda_{\min}(Q)\|Z\|^2}_{c} + 2\frac{\lambda_{\max}^2(P)\|\Xi\|^2}{\lambda_{\min}(Q)}. \tag{54}$$

We would like to relate (c) to V by considering

$$V \leq \lambda_{\max}(P)\|Z\|^2. \tag{55}$$

Now, Eq. (54) can be rewritten as

$$\dot{V} \leq -\alpha V + \left[\alpha\lambda_{\max}(P) - \frac{1}{2}\lambda_{\min}(Q)\right]\|Z\|^2 + 2\frac{\lambda_{\max}^2(P)\|\Xi\|^2}{\lambda_{\min}(Q)}. \tag{56}$$

Pick $\alpha < \frac{\lambda_{\min}(Q)}{2\lambda_{\max}(P)}$, then we have

$$\dot{V} \leq -\alpha V + 2\frac{\lambda_{\max}^2(P)\|\Xi\|^2}{\lambda_{\min}(Q)}. \tag{57}$$

https://doi.org/10.1017/S0263574716000588 Published online by Cambridge University Press

As a result, $\dot{V} < 0$ whenever

$$(\xi, \dot{\xi}, ..., \xi^{(p-1)}, \wp(t)) \in E \equiv \left\{ V > 2\frac{\lambda_{\max}^2(P)}{\alpha\lambda_{\min}(Q)} \sup_{\tau \geq t_0} \|\Xi(\tau)\|^2 \right\}. \tag{58}$$

This implies that $(\xi, \dot{\xi}, ..., \xi^{(p-1)}, \wp(t))$ is uniformly ultimately bounded. Note that the size of the set E is adjustable by proper selection of α ,P and Q . Smaller size of E implies more accuracy in the output tracking.

Until now, we have demonstrated the boundedness of the closed-loop system. It should be mentioned that in practical implementations, the transient performance is also of great importance. Solving Eq. (57) yields

$$V(t) \leq e^{-\alpha(t-t_0)}V(t_0) + 2\frac{\lambda_{\max}^2(P)}{\alpha\lambda_{\min}(Q)} \sup_{t_0 \leq \tau \leq t} \|\Xi(\tau)\|^2. \tag{59}$$

Therefore, according to the lower bound of Lyapunov function, we have

$$\|Z\| \leq \sqrt{\frac{V(t_0)}{\lambda_{\min}(P)}} e^{\frac{-\alpha(t-t_0)}{2}} + \sqrt{\frac{2\lambda_{\max}^2(P)}{\alpha\lambda_{\min}(P)\lambda_{\min}(Q)}} \sup_{t_0 \leq \tau \leq t} \|\Xi(\tau)\| \tag{60}$$

that means the tracking error is bounded by a weighted exponential function plus a constant. This also implies that by adjusting the controller parameters, we may improve the tracking error convergence rate. As a consequence,

$$\lim_{t \to \infty} \|Z\| \leq \sqrt{\frac{2\lambda_{\max}^2(P)}{\alpha\lambda_{\min}(P)\lambda_{\min}(Q)}} \sup_{t_0 \leq \tau \leq t} \|\Xi(\tau)\|. \tag{61}$$

Using the Assumptions (1) and (3) and boundedness of $\|Z\|$, it can be concluded from the stability of the closed-loop system (46) and (49) that the task-space velocity vector $\dot{h}$ is bounded. Since $\dot{q} = J(q)^{-1}\dot{h}$, it follows that $q = \int_0^t J(q)^{-1}\dot{h}dt + q(0)$. Therefore, for finite operational times, the joint position q is bounded.

5. Simulation Results

In this section, simulations results for a six-DOF manipulator are illustrated to verify the satisfactory performance of the proposed controller. The arm which consists of six joints is used to perform the proposed task-space control law. The proposed control scheme is simulated using a Puma560 robot manipulator with the symbolic representation shown in ref. [30]. The Puma robot uses two different sizes of motors—one for the base axes (joints 1–3) and the other for the wrist axes (joints 4–6).[31] The Denavit–Hartenberg (DH) parameters are given in Table I. The robot dynamical parameters are detailed in ref. [32]. The actuator parameters are selected as

$B = diag(1.48 \times 10^{-3}, 817 \times 10^{-6}, 1.38 \times 10^{-3}, 71.2 \times 10^{-6}, 82.6 \times 10^{-6}, 36.7 \times 10^{-6})$
$[N.m.s/rad]$, $R = diag(1.6, 1.6, 1.6, 3.76, 3.76, 3.76)[\Omega]$,
$J_m = diag(2 \times 10^{-4}, 2 \times 10^{-4}, 2 \times 10^{-4}, 33 \times 10^{-6}, 33 \times 10^{-6}, 33 \times 10^{-6})[kg.m^2]$,
$K_b = K_m = diag(0.26, 0.26, 0.26, 0.09, 0.09, 0.09)[N.m/A]$,
$r^{-1} = diag(62.611, 107.82, 53.706, 76.036, 71.923, 76.686)$.

We have chosen roll, pitch and yaw angles for representing the orientation of the end-effector. The transformation matrix is given by

$$[R] = R_z(\alpha)R_y(\beta)R_x(\gamma) = \begin{bmatrix} c_\alpha c_\beta & c_\alpha s_\beta s_\gamma - s_\alpha c_\gamma & c_\alpha s_\beta c_\gamma + s_\alpha s_\gamma \\ s_\alpha c_\beta & s_\alpha s_\beta s_\gamma + c_\alpha c_\gamma & s_\alpha s_\beta c_\gamma - c_\alpha s_\gamma \\ -s_\beta & c_\beta s_\gamma & c_\beta c_\gamma \end{bmatrix}, \tag{62}$$

https://doi.org/10.1017/S0263574716000588 Published online by Cambridge University Press

Table I. Kinematic constant.

Joint i	$d_i(m)$	$a_i(m)$	$\alpha_i(rad)$	θ_i(rad)
1	0	0	$\pi/2$	θ_1
2	0	0.4318	0	θ_2
3	0.15005	0.0203	$-\pi/2$	θ_3
4	0.4318	0	$\pi/2$	θ_4
5	0	0	$-\pi/2$	θ_5
6	0	0	0	θ_6

where c stands for the cosine function, s represents the sine function, $R_x(\gamma)$, $R_y(\beta)$ and $R_z(\alpha)$ are the basic rotation matrices around the three coordinate axes, respectively. Rotation around the axis z by an angle of α is called roll. Also, rotation around the axis y by an angle β is called pitch and rotation around the axis x by an angle of γ is called yaw. In addition, we assume that the end-effector position can be obtained from a position sensor, such as vision systems, electromagnetic measurement systems, position sensitive detectors or laser trackers. The maximum voltage of each motor is set to $u_{\max} = 40\,volt$.[31] It must be emphasized that the dynamic parameters in $M(h)$, $G(h)$, $H(h, \dot{h})$ and the actuator dynamic coefficient matrices are assumed to be unknown. Similarly, the Jacobian matrix $J(q)$ is not exactly known due to uncertainties in robot kinematics. In other words, it is assumed that we are encountering a black box. Now, simulation results relative to two different case studies are presented.

Simulation1: Simple trajectory and robustness evaluation. The performance of the proposed control law is illustrated. The desired end-effector trajectory is a circle with the radius of 0.05m, as

$$\begin{cases} x_d(t) = 0.5 + 0.05\cos(\pi t) \\ y_d(t) = 0.05\sin(\pi t) \\ z_d(t) = 0.5 + 0.05\cos(\pi t) \end{cases} \tag{63}$$

with $\gamma = 1.57$, $\beta = 0.785$ and $\alpha = 0$. The initial joint configuration of the robot is set to $q(0) = [\,2.8653\ 1.8485\ -0.5478\ -1.4953\ 1.3047\ -1.0655\,]^T$ and the initial end-effector position is $x(0) = [\,0.55\ 0\ 0.55\ 1.57\ 0.785\ 0\,]^T$. The external disturbance is defined as

$$T_l(t) = [40.8sin(3.9t) + 27.2sin(5.65t) + 40.8]_{6\times 1} \tag{64}$$

which is applied to all motors. The parameters for the control subsystems are determined as identical primarily, and then, necessary small tunings are made according to the respective simulation results. The design parameters were selected as $k = [\,8000\ 80\,]$, $p = 1$ and $\mu = [\,249.5563\ 5.2411\ 0.0213\,]$. These choices guarantee well-damped behavior of the closed-loop system. It is further assumed that there exist such system uncertainties as 30% in the Jacobian matrix. The actual motions in the x–y–z planes tracked by the proposed method are shown in Fig. 1. As mentioned before, the robotic system should track the modified signal to make the tracking error as small as possible. This signal has been also illustrated in this figure. Figure 2 indicates norm of tracking error in the task-space. Figure 2 shows that the proposed control strategy can effectively attenuate the lumped uncertainties, and improve the tracking accuracy of the end-effector. According to this figure, the maximum tracking error in the x–y–z space is bounded and ignorable. Also, the yaw-pitch-roll errors reduce with acceptable rate. The control efforts, which are produced by the proposed approach and acting on the related joints, are shown in Fig. 3. As shown in this figure, motor voltages are smooth and do not exceed the maximum permitted voltages. From the above simulation results, it is concluded that the control strategy can achieve a favorable control performance and has high robustness.

Simulation 2: Highly complex trajectory. To show the capability of the proposed controller in tasks where precise tracking of fast and complex trajectories is required, we used a second desired

https://doi.org/10.1017/S0263574716000588 Published online by Cambridge University Press

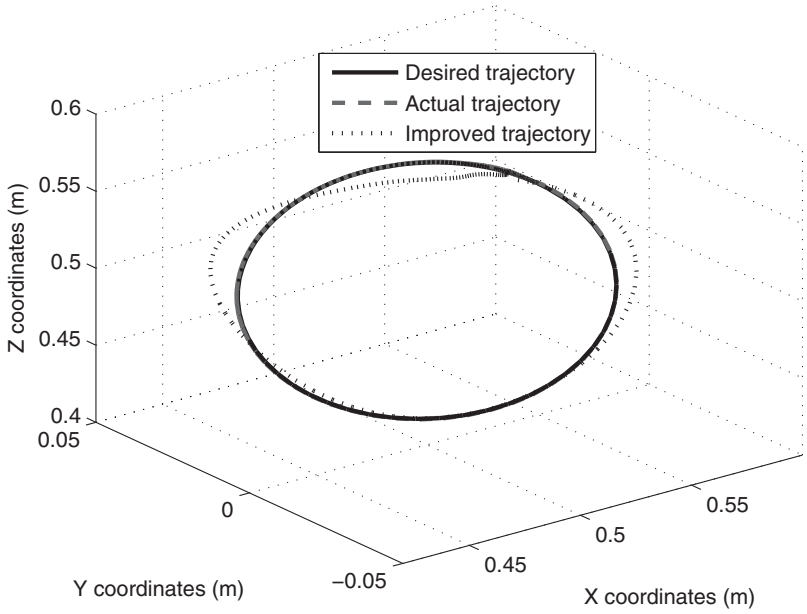


Fig. 1. Following trajectory of the circle motion.

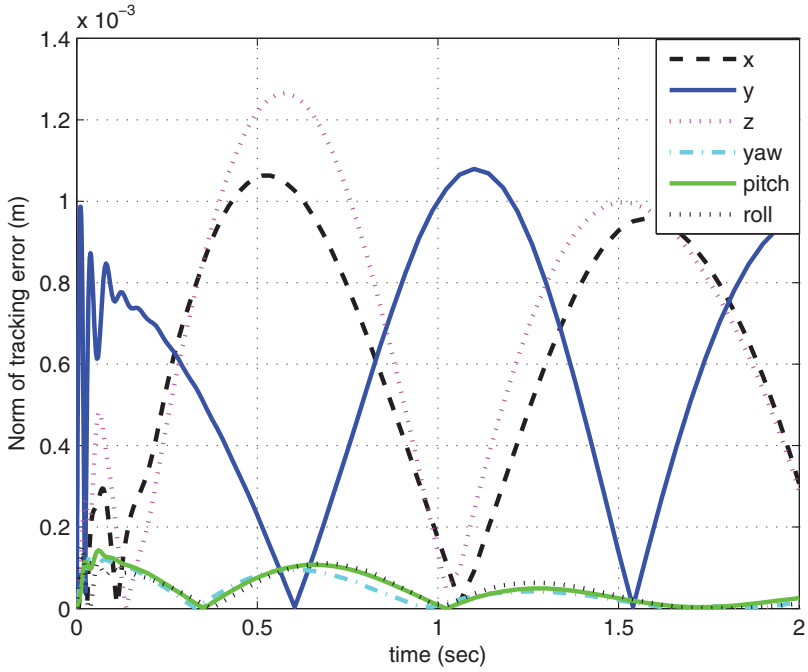


Fig. 2. Norm of tracking error.

trajectory generated by

$$\begin{cases} x_d(t) = 0.5 + 0.02sin\,(4t) + 0.02sin\,(24t) \\ y_d(t) = 0.26 + 0.02sin\,(4t + 1.6) + 0.02sin\,(24t + 1.6) \\ z_d(t) = 0 \end{cases}, \tag{65}$$

where the initial manipulator configuration is $q(0) = [3.4218 \quad 2.2805 \quad 0.1971 \quad -1.348 \quad 1.742 \quad 0.1406]^T$. This trajectory is very important, since it involves rapid and complex reactions between different dynamics of the manipulator. The controller parameters are selected as $k = [\,10000 \;\; 100\,]$,

https://doi.org/10.1017/S0263574716000588 Published online by Cambridge University Press

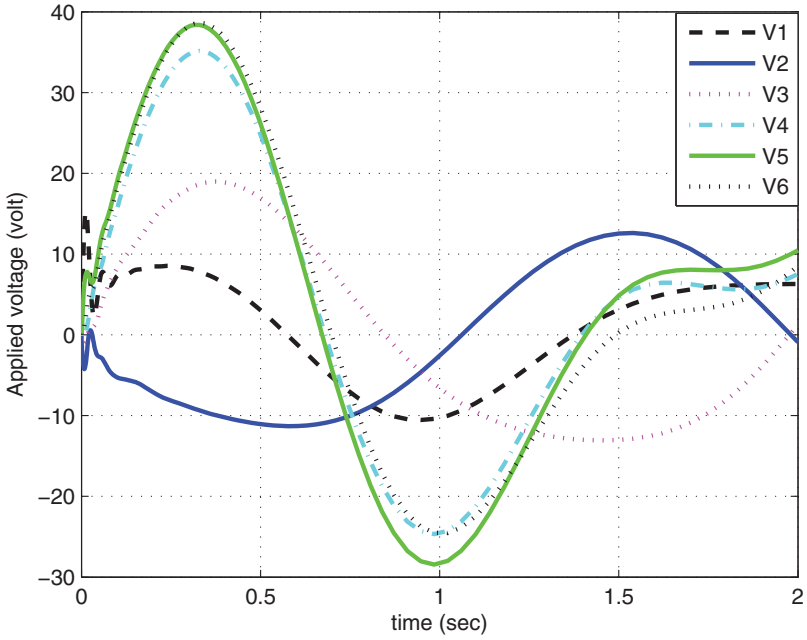


Fig. 3. Motor voltages.

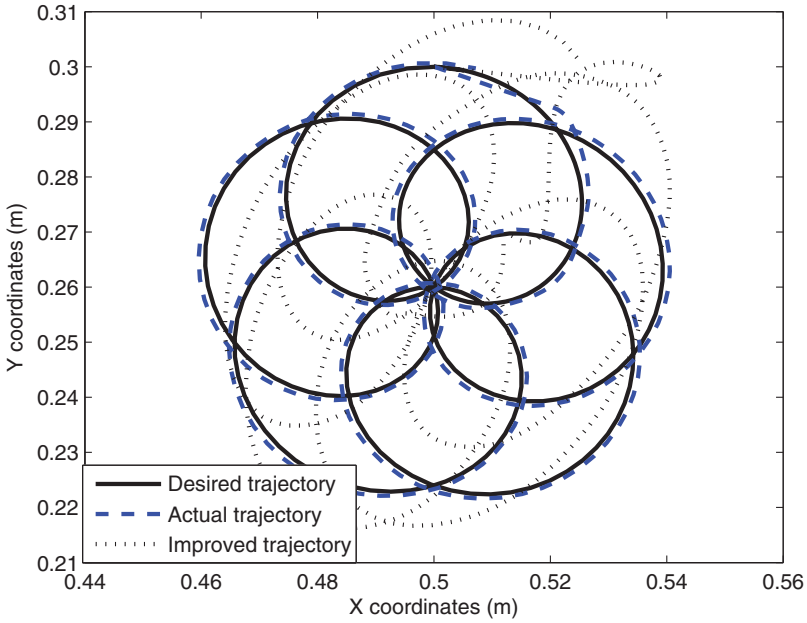


Fig. 4. Tracking response.

$p = 1$ and $\mu = [\,500.0231\ 5.2413\ 0.0213\,]$. The external disturbance is chosen as

$$T_l(t) = \begin{bmatrix} 40.8sin(\pi t) + 27.2sin(6\pi t) + 40.8 \\ 28.56sin(2\pi t) + 19.4sin(5\pi t) + 28.56 \\ 20.4sin(3\pi t) + 13.6sin(4\pi t) + 20.4 \\ 18.36sin(4\pi t) + 12.24sin(3\pi t) + 18.36 \\ 8.16sin(5\pi t) + 5.44sin(2\pi t) + 8.16 \\ 24.48sin(6\pi t) + 16.32sin(\pi t) + 24.48 \end{bmatrix}. \tag{66}$$

https://doi.org/10.1017/S0263574716000588 Published online by Cambridge University Press

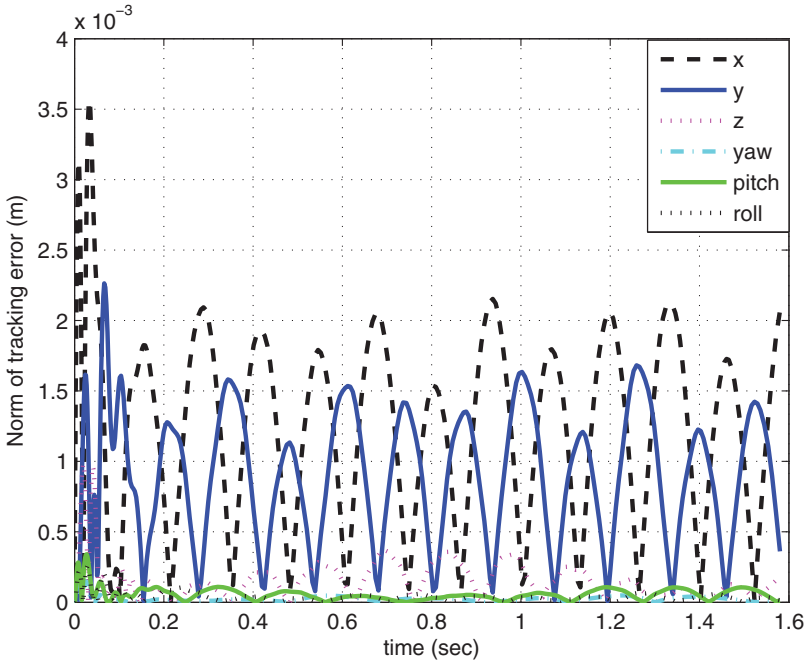


Fig. 5. Norm of tracking error.

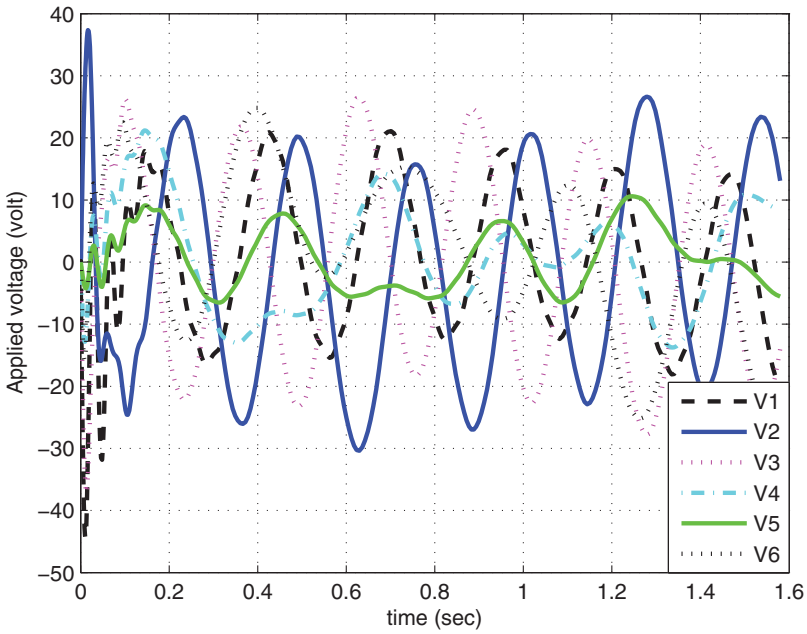


Fig. 6. Motor voltages.

The results of this simulation are shown in Figs. 4 through 6. The tracking performance of the endpoint is illustrated in Fig. 4. According to Eq. (50), the robotic system should track the modified signal to make the tracking error as small as possible. This signal has been also illustrated in this figure. According to this figure, the controller is capable of overcoming various uncertainties including external disturbances on the motors shafts, and modeling error in tracking fast and complex trajectories with negligible tracking errors. Figure 5 shows norms of tracking error in the operational space. As shown in this figure, the maximum tracking error in the x–y–z space occurs at initial times due to the high speed of the desired trajectory and reduces immediately. The applied input voltage for the joint actuators has also been shown in Fig. 6. It can be observed from the above results that the

https://doi.org/10.1017/S0263574716000588 Published online by Cambridge University Press

robot's end-effector successfully follows complex predetermined trajectories, and the system stability is guaranteed, even in the case where no knowledge of the system is in hand.

6. Conclusion

A robust task-space control strategy has been proposed for electrically driven robots. The control laws have been derived under the assumption that no information of the system is in hand. The system stability has been verified by the Lyapunov method. Simulation results have demonstrated the effectiveness of the control. The important feature of the proposed scheme consists in the simplicity of the control laws, which do not contain explicit information of the system, actuators and Jacobean matrix. It has been shown that the control system is robust with the presence of uncertainties including modeling errors and external disturbances.

References

1. M. W. Spong, "On the robust control of robot manipulators," *IEEE Trans. Autom. Control* **37**, 1782–1786 (1992).
2. L. Bascetta and P. Rocco, "Revising the robust control design for rigid robot manipulators," *IEEE Trans. Robot.* **26**, 180–187 (2010).
3. M. M. Fateh and S. Khorashadizadeh, "Optimal Robust voltage control of electrically driven robot manipulators," *Nonlinear Dyn*. **70**, 1445–1458 (2012).
4. A. Izadbakhsh and M. M. Fateh, "Robust Lyapunov-based control of flexible-joint robots using voltage control strategy," *Arab J. Sci. Eng.* **39**, 3111–3121 (2014).
5. A.-C. Huang and M.-C. Chien, *Adaptive Control of Robot Manipulators: A Unified Regressor Free Approach*, World Scientific Publishing Co. Pte. Ltd. Singapore (World Science, 2010).
6. S. Islam and P. Liu, "Robust sliding mode control for robot manipulators," *IEEE Trans. Ind. Electron.* **58**, 2444–2453 (2011).
7. E. Kim, "Output feedback tracking control of robot manipulators with model uncertainty via adaptive fuzzy logic," *IEEE Trans. Fuzzy Syst.* **12**, 368–378 (2004).
8. M. M. Fateh and S. Khorashadizadeh, "Robust control of electrically driven robots by adaptive fuzzy estimation of uncertainty," *Nonlinear Dyn*. **69**, 1465–1477 (2012).
9. S. Puga-Guzmán, J. M. Valenzuela and V. Santibáñez, "Adaptive neural network motion control of manipulators with experimental evaluations," *The Sci. World J.*, doi: 10.1155/2014/694706 (2014).
10. L. X. Wang, *A Course in Fuzzy Systems and Control* (Prentice-Hall, New York, 1997)
11. A. Izadbakhsh, "Robust control design for rigid-link flexible-joint electrically driven robot subjected to constraint: Theory and experimental verification," *Nonlinear Dyn*. **85**, 751–765 (2016).
12. M.-C. Chien and A.-C. Huang, "Adaptive impedance controller design for flexible-joint electrically-driven robots without computation of the regressor matrix," *Robotica* **30**, 133–144 (2012).
13. Y. C. Tsai and A.-C. Huang, "FAT based adaptive control for pneumatic servo system with mismatched uncertainties," *Mech. Syst. Sig. Process.* **22**, 1263–1273 (2008).
14. A.-C. Huang and Y. S. Kuo, "Sliding control of nonlinear systems containing time-varying uncertainties with unknown bounds," *Int. J. Control* **74**, 252–264 (2001).
15. M.-C. Chien and A.-C. Huang, "Adaptive impedance control of robot manipulators based on function approximation technique," *Robotica* **22**, 395–403 (2004).
16. A.-C. Huang, S. C. Wu and W. F. Ting, "An FAT-based adaptive controller for robot manipulators without regressor matrix: Theory and experiments," *Robotica* **24**, 205–210 (2006).
17. S. Khorashadizadeh and M. M. Fateh, "Uncertainty estimation in robust tracking control of robot manipulators using the fourier series expansion," *Robotica* DOI: http://dx.doi.org/10.1017/S026357471500051X (2015).
18. S. Khorashadizadeh and M. M. Fateh, "Adaptive Fourier Series-Based Control of Electrically Driven Robot Manipulators," *The 3rd International Conference on Control, Instrumentation, and Automation (ICCIA)*, (Tehran, 2013) pp. 213–218.
19. S. Khorashadizadeh and M. M. Fateh, "Robust task-space control of robot manipulators using Legendre polynomials for uncertainty estimation," *Nonlinear Dyn*. **79**, 1151–1161 (2014).
20. S. E. Talole, J. P. Kolhe and S. B. Phadke, "Extended-state-observer-based control of flexible-joint system with experimental validation," *IEEE Trans. Ind. Electron.* **57**, 1411–1419 (2010).
21. C. C. Cheah, C. Liu and J. J. E. Slotine, "Adaptive jacobian tracking control of robots with uncertainties in kinematic, dynamic and actuator models," *IEEE Trans. Autom. Control* **51**, 1024–1029 (2006).
22. A. Izadbakhsh and M. M. Fateh, "Real-time robust adaptive control of robots subjected to actuator voltage constraint," *Nonlinear Dyn*. **78**, 1999–2014 (2014).
23. J. Moreno-Valenzuela, R. Campa and V. Santibáñez, "Model-based control of a class of voltage-driven robot manipulators with non-passive dynamics," *Comput. Electr. Eng.* **39**, 2086–2099 (2013).
24. J. Orrante-Sakanassi, V. Santibañez and J. Moreno-Valenzuela, "Stability analysis of a voltage-based controller for robot manipulators," *Int. J. Adv. Robot. Syst.* doi: 10.5772/53894 (2013).

https://doi.org/10.1017/S0263574716000588 Published online by Cambridge University Press

25. O. Khatib, "A unified approach for motion and force control of robot manipulators: The operational space formulation," *IEEE J. Robot. Autom.* **3**, 43–53 (1987).
26. A. Izadbakhsh and S. M. R. Rafiei, "Endpoint perfect tracking control of robots-a robust non inversion-based approach," *Int. J. Control Autom. Syst.* **7**, 888–898 (2009).
27. A. Izadbakhsh, A. Akbarzadeh Kalat, M. M. Fateh and S.M.R. Rafiei, "A robust anti-windup control design for electrically driven robots-theory and experiment," *Int. J. Control Autom. Syst.* **9**, 1005–1012 (2011).
28. A. Izadbakhsh and S. M. R. Rafiei, "Robust Control Methodologies for Optical Micro Electro Mechanical System-New Approaches and Comparison," *13th Power Electronics and Motion Control Conference on EPE-PEMC*, (Poznan, 2008) pp. 2102–2107.
29. W. Rudin, *Principles of Mathematical Analysis*, McGraw-Hill Education; 3rd edition (January 1, 1976).
30. A. Izadbakhsh, "Closed-form Dynamic Model of Puma560 Robot Arm," *Proceedings of the 4th International Conference on Autonomous Robots and Agents*, (Wellington, 2009) pp. 675–680.
31. P. Corke, "The Unimation Puma Servo System," *CSIRO Division of Manufacturing Technology*, (1994) p. 38.
32. P. Corke and B. Armstrong-Helouvry, "A Search for Consensus Among Model Parameters Reported for the Puma560 Robot," *IEEE International Conference on Robotics and Automation*, (San Diego, CA, 1994) pp. 1608–1613.

https://doi.org/10.1017/S0263574716000588 Published online by Cambridge University Press